

Article

# Isolation, Structure Elucidation, and Antiproliferative Activity of Butanolides and Lignan Glycosides from the Fruit of *Hernandia nymphaeifolia*

Simayijiang Aimaiti <sup>1</sup>, Yohei Saito <sup>1</sup>, Shuichi Fukuyoshi <sup>1</sup>, Masuo Goto <sup>2</sup>, Katsunori Miyake <sup>3</sup>, David J. Newman <sup>4</sup>, Barry R. O'Keefe <sup>5,6</sup>, Kuo-Hsiung Lee <sup>2,7</sup> and Kyoko Nakagawa-Goto <sup>1,2,\*</sup>

- <sup>1</sup> School of Pharmaceutical Sciences, College of Medical, Pharmaceutical and Health Sciences, Kanazawa University, Kanazawa 920-1192, Japan; ismayil507@stu.kanazawa-u.ac.jp (S.A.); saito-y@staff.kanazawa-u.ac.jp (Y.S.); fukuyosi@p.kanazawa-u.ac.jp (S.F.)
- <sup>2</sup> Natural Products Research Laboratories, UNC Eshelman School of Pharmacy, University of North Carolina at Chapel Hill, Chapel Hill, NC 27599-7568, USA; goto@med.unc.edu (M.G.); khlee@unc.edu (K.-H.L.)
- <sup>3</sup> Tokyo University of Pharmacy and Life Sciences, Hachioji, Tokyo 192-0392, Japan; miyake@toyaku.ac.jp
- <sup>4</sup> NIH Special Volunteer, Wayne, PA 19087, USA; newmand@mail.nih.gov
- <sup>5</sup> Natural Products Branch, Developmental Therapeutics Program, Division of Cancer Treatment and Diagnosis, National Cancer Institute, NCI at Frederick, Frederick, MD 21702-1201, USA; okeefeba@mail.nih.gov
- <sup>6</sup> Molecular Targets Program, Center for Cancer Research, National Cancer Institute, NCI at Frederick, Frederick, MD 21702-1201, USA
- <sup>7</sup> Chinese Medicine Research and Development Center, China Medical University and Hospital, Taichung 40447, Taiwan
- \* Correspondence: kngoto@p.kanazawa-u.ac.jp; Tel.: +81-762-264-6305

Academic Editor: Maria Carla Marcotullio

Received: 9 October 2019; Accepted: 31 October 2019; Published: 5 November 2019



**Abstract:** Seven new butanolides, peltanolides A–G (1–7), and two lignan glucosides, peltasides A (8) and B (9), along with eleven known compounds, 10–20, were isolated from a crude CH<sub>3</sub>OH/CH<sub>2</sub>Cl<sub>2</sub> (1:1) extract of the fruit of *Hernandia nymphaeifolia* (Hernandiaceae). The structures of 1–9 were characterized by extensive 1D and 2D NMR spectroscopic and HRMS analysis. The absolute configurations of newly isolated compounds 1–9 were determined from data obtained by optical rotation and electronic circular dichroism (ECD) exciton chirality methods. Butanolides and lignan glucosides have not been isolated previously from this genus. Several isolated compounds were evaluated for antiproliferative activity against human tumor cell lines. Lignans 15 and 16 were slightly active against chemosensitive tumor cell lines A549 and MCF-7, respectively. Furthermore, both compounds displayed significant activity (IC<sub>50</sub> = 5 μM) against a P-glycoprotein overexpressing multidrug-resistant tumor cell line (KB-VIN) but were less active against its parent chemosensitive cell line (KB).

**Keywords:** *Hernandia nymphaeifolia*; butanolides; lignan glycosides; antiproliferative activity

## 1. Introduction

Plants in the genus *Hernandia* (Hernandiaceae) are found in subtropical and tropical areas [1]. They contain diverse bioactive secondary metabolites, especially lignans, including podophyllotoxin analogues [2,3], and benzylisoquinolines [4], including aporphines [5–7]. These compounds exhibit various biological activities, including significant cytotoxic [8,9], antiplasmodial [9,10], and antibacterial activities [2]. *H. nymphaeifolia* (C.Presl) Kubitzki (synonym: *H. peltata* Meisn.) is a common coastal tree and grows to 12–20 m in height. This plant has been used for the treatment of abdominal

pains, boils, cough, diarrhea, eye problems, and convulsions as a traditional medicine in western Samoa [11]. A CH<sub>3</sub>OH/CH<sub>2</sub>Cl<sub>2</sub> (1:1) extract of *H. nymphaeifolia* (N053499, originally described as *H. peltata*) provided by the U.S. National Cancer Institute Natural Products Branch (NCI, Frederick, MD, USA) exhibited broad cytotoxicity in the NCI-60 human tumor cell line (HTCL) assay, possibly due to the above or similar cytotoxic constituents. To supplement the reported phytochemical research on *H. nymphaeifolia* [2,4,9,12–14], we conducted a thorough study to identify new chemical compounds as part of our continuing investigation of rainforest plants. Accordingly, the extract of N053499 yielded seven new butanolides, peltanolides A–G (1–7), and two new lignan glycosides, peltasides A (8) and B (9), as well as eleven known compounds 10–20 (Figure 1). Herein, we report the details of isolation, structure elucidation, and cytotoxicity of isolated compounds from *H. nymphaeifolia*.

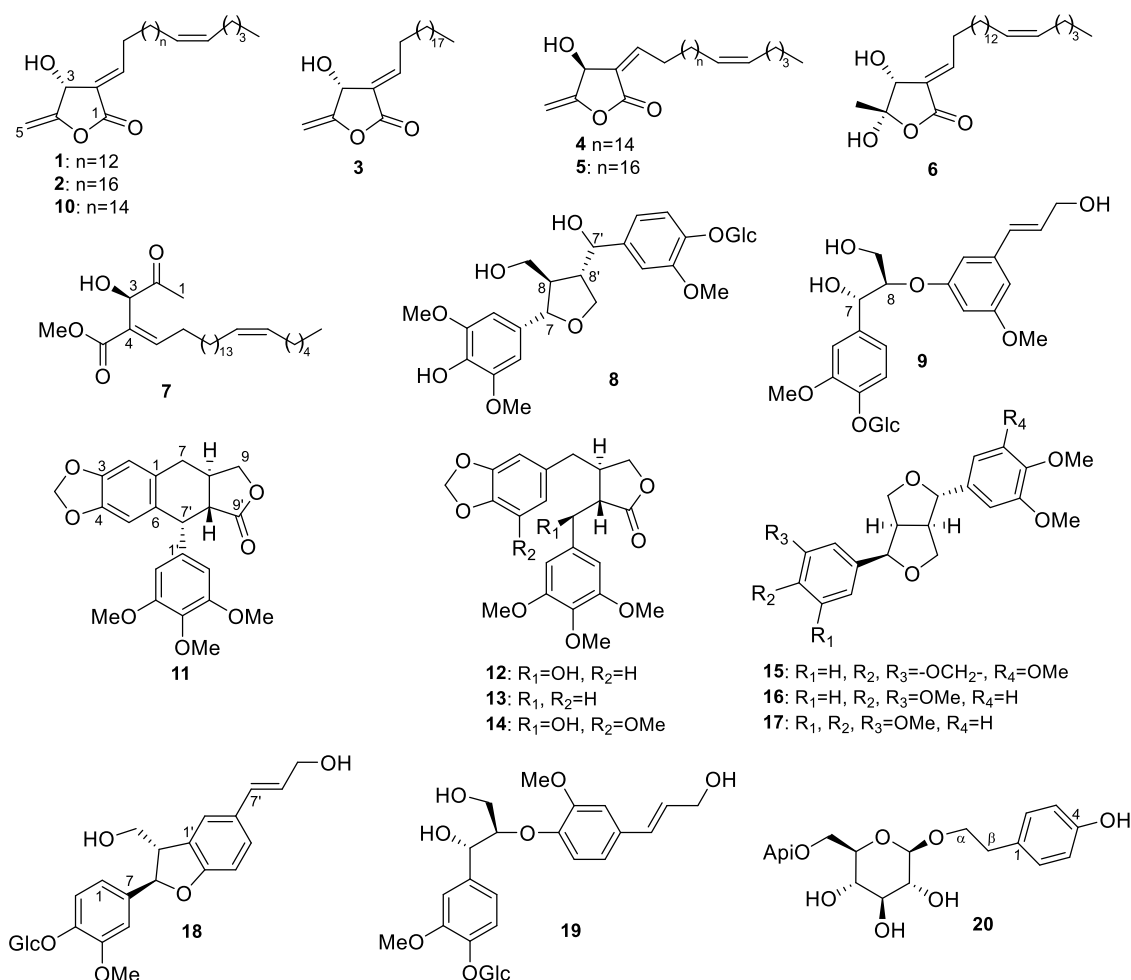


Figure 1. Isolated compounds (1–20) from *H. nymphaeifolia*.

## 2. Results and Discussion

### 2.1. Structure Elucidation of Isolated Compounds from *H. nymphaeifolia*

The CH<sub>3</sub>OH/CH<sub>2</sub>Cl<sub>2</sub> (1:1) extract of *H. nymphaeifolia* (fruit, N053499) was firstly partitioned with water and *n*-hexane. The water fraction was further partitioned with EtOAc and *n*-BuOH. All fractions were subjected to a combination of column chromatography, preparative HPLC, and preparative TLC using silica gel and octadecylsilyl (ODS) to give seven new butanolides, peltanolides A–G (1–7), and two new lignan glycosides, peltasides A (8) and B (9), as well as eleven known compounds, tambouranolide (10) [15], deoxypodophyllotoxin (11) [16], podorhizol (12) [17], bursehernin (13) [18], (2*S*,3*S*)-(+)-5'-methoxyatein (14) [19], epiashantin (15) [20], epiuedesmin (16) [21], (1*S*,3*aR*,4*R*,6*aR*)-

1-(3,4-dimethoxyphenyl)-4-(3',4',5'-trimethoxyphenyl)tetrahydro-1*H*,3*H*-furo-[3-*c*]furan (**17**) [20], (7*R*,8*S*)-dehydrodiconiferyl alcohol-4-*O*- $\beta$ -*D*-glucoside (**18**) [22], alacchanoside A (**19**) [23], and osmanthuside H (**20**) [24]. The structures of all known compounds were identified by comparison of their spectroscopic data with reported values.

Compound **1** was obtained as a yellow amorphous solid:  $[\alpha]_D^{25} + 27.3$  (*c* 0.075, CHCl<sub>3</sub>). It gave a  $[M]^+$  peak at *m/z* 390.3137, appropriate for a molecular formula of C<sub>25</sub>H<sub>42</sub>O<sub>3</sub>. The <sup>1</sup>H and <sup>13</sup>C NMR spectra (Tables 1 and 2) contained signals attributed to oxymethine [ $\delta_H$  5.26 (1H, brs);  $\delta_C$  66.5, C-3], methyldiene [ $\delta_H$  4.96 (1H, dd, *J* = 2.8, 1.4 Hz), 4.72 (1H, dd, *J* = 2.8, 1.4 Hz);  $\delta_C$  91.4, 157.6, C-4,5], vinyl [ $\delta_H$  7.09 (1H, td, *J* = 7.8, 2.2 Hz);  $\delta_C$  127.3, 150.3, C-2,6], and carbonyl ( $\delta_C$  166.5, C-1) groups, consistent with a  $\beta$ -hydroxy- $\gamma$ -methylene- $\alpha,\beta$ -unsaturated- $\gamma$ -lactone. The chemical shifts of H-6 ( $\delta_H$  7.09) and H-7 ( $\delta_H$  2.48) as well as allylic carbon C-3 ( $\delta_C$  66.5) and olefinic carbon C-6 ( $\delta_C$  150.3) were identical with those of tambouranolide (**10**) [15] and related linderanolides and isolinderanolides [25,26] with an *E*-configured double bond [ $\Delta^{2(6)}$ ]. This assignment was also supported by a cross-peak between H-3 and H-7 in the NOESY spectrum (Figure 3). The presence of a long aliphatic chain containing a double bond was suggested by NMR resonances for olefinic and multiple methylene carbons. The allylic ( $\delta_C$  27.0, 27.2) and olefinic ( $\delta_C$  129.8, 129.9) carbon signals in the <sup>13</sup>C NMR spectrum of **1** suggested that the internal olefin has the typical *Z*-configuration, comparable with those of **10** as well as the abovementioned linderanolides and isolinderanolides with *Z*-double bonds in the side chain. In a related *E*-isomer, the allylic and olefinic carbons appeared at 32.6 and 25.6 ppm and at 131.9 and 129.3 ppm, respectively [25]. The location of the olefinic bond at  $\Delta^{20}$  was based on HMBC and COSY correlations (Figure 2). From the NMR and HREIMS data, compounds **10** and **1** differ only in the number of methylene groups (16 in **10**, 14 in **1**) in the long aliphatic chain. The absolute configuration of **1** was determined from its optical rotation, which was the same as that of **10**. Furthermore, the total synthesis of peumusolide A analogues clearly proved that the optical rotation is positive for 3*R* compounds and negative for 3*S* [27,28]. Therefore, compound **1** (peltanolide A) was assigned as (2*E*,3*R*)-3-hydroxy-4-methylidene-2-[(15*Z*)-15-icosenylidene]butanolide.

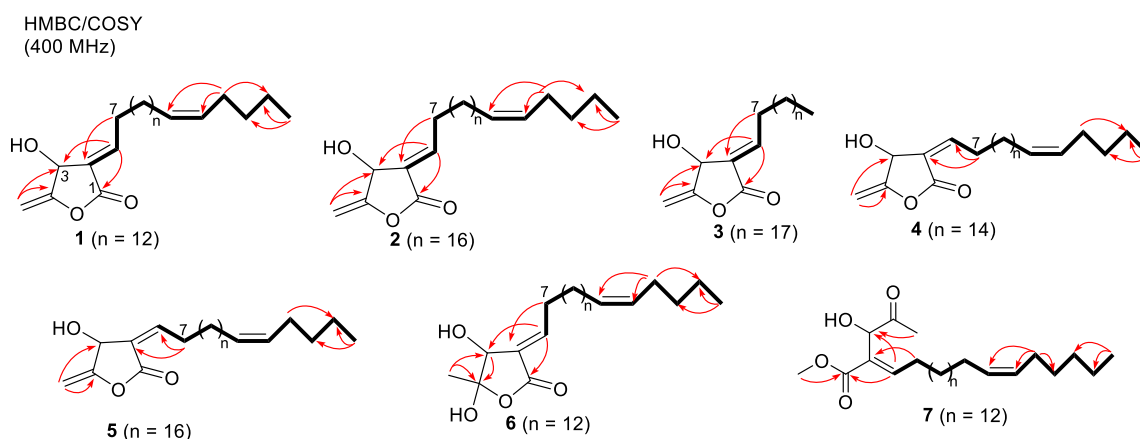


**Figure 2.** Selected HMBC correlations (arrows in red), COSY connectivities (bold lines) for compounds **1–7**.

Compound **2** was isolated as a yellow solid,  $[\alpha]_D^{25} + 26.1$  (*c* 0.12, CHCl<sub>3</sub>). The HREIMS data supported a molecular formula of C<sub>29</sub>H<sub>51</sub>O<sub>3</sub> from the peak at *m/z* 446.3743  $[M]^+$ . The MS data and NMR spectra indicated four additional methylene units compared with **1**, and the optical rotation suggested the same configuration as that of **1**. Thus, compound **2** (peltanolide B) was defined as (2*E*,3*R*)-3-hydroxy-4-methylidene-2-[(19*Z*)-19-tetracosenylidene]butanolide.

Compound **3** was obtained as a colorless oil:  $[\alpha]_D^{25} + 26.0$  (*c* 0.07, CHCl<sub>3</sub>). The HREIMS data indicated a molecular formula of C<sub>25</sub>H<sub>44</sub>O<sub>3</sub> from the peak at *m/z* 392.3302  $[M]^+$ , which was identical to that of miaolinolide [29]. One dimensional NMR spectra of **3** also displayed the similar signal

pattern with one exception: the chemical shift of H-6 is  $\delta_{\text{H}}$  7.10 (1H, td,  $J = 7.8, 2.2$  Hz) in **3** and  $\delta_{\text{H}}$  6.70 (1H, td,  $J = 8.0, 2.0$  Hz) in miaolinolide. Thus, the  $\Delta^{2(6)}$  double bond has an *E* configuration in **3**, rather than the *Z* configuration in miaolinolide [29]. This assignment was also proved that the chemical shift of H-6 in **3** was close to that of related butanolides with an *E* configuration of the  $\Delta^{2(6)}$  double bond [15,25,26,30], including compounds **1** and **2**. A NOESY correlation between H-3 and H-7 (Figure 3) supported this conclusion. Based on their optical rotations, compound **3** and miaolinolide have the same absolute configuration. Hence, the structure of **3** (peltanolide C) was established as (2*E*,3*S*)-3-hydroxy-4-methylidene-2-icosylidenebutanolide.

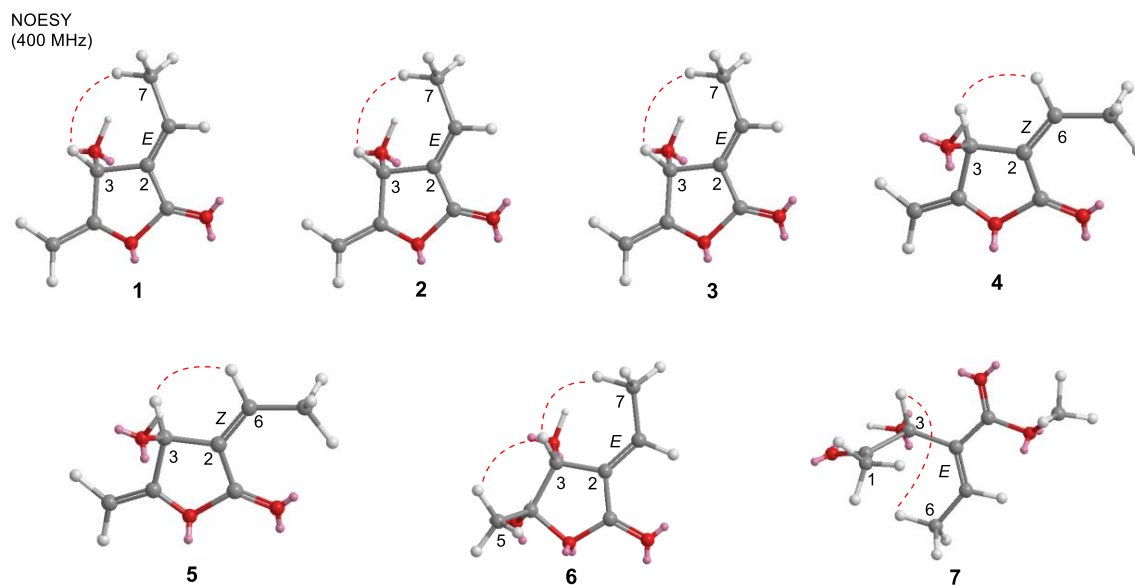


**Figure 3.** Key NOESY (red dashed lines) correlations for compounds 1–7.

HRFABMS of compound **4** showed a molecular formula  $\text{C}_{27}\text{H}_{46}\text{O}_3$  with a molecular ion at  $m/z$  441.3357  $[\text{M} + \text{Na}]^+$ . The  $^1\text{H}$  and  $^{13}\text{C}$  NMR spectra of **4** (Tables 1 and 2) were comparable to those of **10** but suggested different double bond  $[\Delta^{2(6)}]$  configurations and C-3 stereochemistries. For **4**, the  $\Delta^{2(6)}$  configuration was determined as *Z* from a NOESY correlation between H-3 and H-6 (Figure 3) and the chemical shift of H-6 at 6.69 ppm rather than ca. 7.10 ppm for the *E* form. The C-3 stereochemistry was determined as *S* by comparison of optical rotations,  $[\alpha]_{\text{D}}^{25} -29.7$  ( $c$  0.02,  $\text{CHCl}_3$ ) for **4** and  $[\alpha]_{\text{D}}^{25} + 18.0$  ( $c$  0.03,  $\text{CHCl}_3$ ) for **10** with 3*R*. Thus, compound **4** (peltanolide D) was determined as (2*Z*,3*S*)-3-hydroxy-4-methylidene-2-[(17*Z*)-17-docosenylidene]butanolide.

Table 1. <sup>1</sup>H NMR Spectroscopic data of compounds 1–7.

	1 <sup>a</sup> (CDCl <sub>3</sub> )	2 <sup>b</sup> (CDCl <sub>3</sub> )	3 <sup>b</sup> (CDCl <sub>3</sub> )	4 <sup>b</sup> (CDCl <sub>3</sub> )	5 <sup>b</sup> (CDCl <sub>3</sub> )	6 <sup>a</sup> (CDCl <sub>3</sub> )	7 <sup>b</sup> (CDCl <sub>3</sub> )
Position	δ <sub>H</sub> (J in Hz)						
1							2.15 s
3	5.26 brs	5.26 brs	5.26 brd (5.6)	5.11 m	5.10 brd (7.3)	4.82 brs	4.89 d (4.2)
5a	4.72 dd (2.8, 1.4)	4.72 dd (2.8, 1.4)	4.72 dd (2.8, 1.4)	4.67 dd (2.8, 1.4)	4.66 dd (2.8, 1.4)	1.62 s	7.07 t (8.0)
5b	4.96 dd (2.8, 1.4)	4.96 dd (2.8, 1.4)	4.96 dd (2.8, 1.4)	4.89 dd (2.8, 1.4)	4.89 dd (2.8, 1.4)		
6	7.09 td (7.8, 2.2)	7.09 td (7.8, 2.2)	7.10 td (7.8, 2.2)	6.69 td (7.8, 2.2)	6.67 td (7.8, 2.2)	7.04 td (7.8, 2.2)	2.34 td (14.8, 8.0)
7	2.48 m	2.48 m	2.48 m, 2.43 m	2.78 m	2.76 m	2.38 m	1.50 m
8	1.52 m	1.52 m	1.53 m	1.46 m	1.45 m	1.52 m	1.25 m <sup>P</sup>
9–18	1.26 m <sup>c</sup>	1.26 m <sup>e</sup>	1.25 m <sup>g</sup>	1.25 m <sup>h</sup>	1.25 m <sup>j</sup>	1.25 m <sup>m</sup>	1.25 m <sup>P</sup>
19	2.00 m	1.26 m <sup>e</sup>	1.25 m <sup>g</sup>	1.25 m <sup>h</sup>	1.25 m <sup>j</sup>	2.01 m <sup>n</sup>	2.00 m <sup>Q</sup>
20	5.36 m <sup>d</sup>	1.26 m <sup>e</sup>	1.25 m <sup>g</sup>	1.25 m <sup>h</sup>	1.25 m <sup>j</sup>	5.34 t (4.8) <sup>o</sup>	5.34 t (4.8) <sup>r</sup>
21	5.36 m <sup>d</sup>	1.26 m <sup>e</sup>	1.25 m <sup>g</sup>	2.02 m	1.25 m <sup>j</sup>	5.34 t (4.8) <sup>o</sup>	5.34 t (4.8) <sup>r</sup>
22	2.02 m	1.26 m <sup>e</sup>	1.25 m <sup>g</sup>	5.35 m <sup>i</sup>	1.25 m <sup>j</sup>	2.01 m <sup>n</sup>	2.00 m <sup>Q</sup>
23	1.26 m <sup>c</sup>	2.00 m	1.25 m <sup>g</sup>	5.35 m <sup>i</sup>	2.01 m <sup>k</sup>	1.25 m <sup>m</sup>	1.25 m <sup>P</sup>
24	1.32 m	5.36 m <sup>f</sup>	1.25 m <sup>g</sup>	2.02	5.33 m <sup>l</sup>	1.31	1.25 m <sup>P</sup>
25	0.89 t (6.9)	5.36 m <sup>f</sup>	0.89 br t (7.3)	1.25 m <sup>h</sup>	5.33 m <sup>l</sup>	0.89 t (6.0)	1.31 m
26		2.02 m		1.33 m	2.01 m <sup>k</sup>		0.89 t (6.0)
27		1.26 m <sup>e</sup>		0.88 t (6.9)	1.25 m <sup>j</sup>		
28		1.32 m			1.32 m		
29		0.89 t (7.3)			0.87 t (6.9)		
2-OH		2.26 m					
3-OH							4.00 brs
OCH <sub>3</sub>							3.72 s

<sup>a</sup> 600 MHz, <sup>b</sup> 400 MHz, <sup>c–r</sup> Overlapping signals.

Table 2.  $^{13}\text{C}$  NMR Spectroscopic data in  $\text{CDCl}_3$  of compounds 1–7.

	<b>1<sup>a</sup></b>	<b>2<sup>b</sup></b>	<b>3<sup>b</sup></b>	<b>4<sup>b</sup></b>	<b>5<sup>b</sup></b>	<b>6<sup>a</sup></b>	<b>7<sup>b</sup></b>
<b>Position</b>	$\delta_c$	$\delta_c$	$\delta_c$	$\delta_c$	$\delta_c$	$\delta_c$	$\delta_c$
1	166.5	166.5	166.3	163.1		166.4	24.8
2	127.3	127.3	127.2	127.4	127.3	125.2	206.3
3	66.5	66.5	66.6	68.9	68.9	70.9	73.4
4	157.6	157.6	157.5	160.1	160.2	100.1	129.8
5	91.4	91.4	91.5	90.3	90.4	26.8	149.0
6	150.3	150.3	150.3	151.4	151.4	151.9	28.7
7	29.8	29.8	29.8	29.8	29.8	30.1	29.3
8	28.4	28.4	28.4–29.6 <sup>d</sup>	28.4	28.4	29.5–29.9 <sup>g</sup>	29.4–30.0 <sup>h</sup>
9–18	29.4–30.0	29.4–30.0 <sup>c</sup>	28.4–29.6 <sup>d</sup>	29.4–30.0 <sup>e</sup>	29.4–30.0 <sup>f</sup>	29.5–29.9 <sup>g</sup>	29.4–30.0 <sup>h</sup>
19	27.0	29.4–30.0 <sup>c</sup>	28.4–29.6 <sup>d</sup>	29.4–30.0 <sup>e</sup>	29.4–30.0 <sup>f</sup>	27.0	27.2
20	129.8	29.4–30.0 <sup>c</sup>	28.4–29.6 <sup>d</sup>	29.4–30.0 <sup>e</sup>	29.4–30.0 <sup>f</sup>	129.8	129.8
21	129.9	29.4–30.0 <sup>c</sup>	28.4–29.6 <sup>d</sup>	27.0	29.4–30.0 <sup>f</sup>	129.9	129.9
22	27.2	29.4–30.0 <sup>c</sup>	28.4–29.6 <sup>d</sup>	129.8	29.4–30.0 <sup>f</sup>	27.7	27.2
23	32.0	27.0	32.0	129.9	27.0	32.1	29.8
24	22.4	129.8	22.8	27.2	129.8	22.5	31.9
25	14.0	129.9	14.1	32.0	129.9	14.1	22.7
26		27.2		22.3	27.2		14.1
27		32.0		14.0	32.0		
28		22.4			22.4		
29		14.0			14.0		
COO							166.5
OCH <sub>3</sub>							52.0

<sup>a</sup> 150 MHz, <sup>b</sup> 100 MHz, <sup>c–h</sup> Overlapping signals.

Compound **5** was obtained as a yellow solid and displayed a peak at  $m/z$  446.3749  $[M]^+$  in the HREIMS spectrum, which agreed with a molecular formula of  $C_{29}H_{50}O_3$  and two additional methylene units ( $C_2H_4$ ) compared with **4**. This finding was also supported by the two NMR spectra. Both compounds also have the same absolute configurations based on their optical rotations,  $[\alpha]^{25}_D$   $-21.1$  ( $c$  0.015,  $CHCl_3$ ) for **5** and  $[\alpha]^{25}_D$   $-29.7$  ( $c$  0.02,  $CHCl_3$ ) for **4**. Thus, compound **5** (peltanolide E) was defined as (2*Z*,3*S*)-3-hydroxy-4-methylidene-2-[(15*Z*)-15-icosenylidene]butanolid.

Compound **6** was isolated as a colorless oil. The HREIMS data indicated a molecular formula of  $C_{25}H_{44}O_4$  from the peak at  $m/z$  408.3230  $[M]^+$ . Compared with **1**, the  $^1H$  and  $^{13}C$  NMR spectra of **6** (Tables 1 and 2) showed the absence of signals for a methylidene group and the presence of signals for a methyl group [ $\delta_H$  1.62 (3H, s)/ $\delta_C$  26.8] and a doubly oxygenated carbon ( $\delta_C$  100.1). The doubly oxygenated carbon was assigned as C-4 with an attached methyl group; these assignments were confirmed by HMBC correlations (Figure 2). A NOESY correlation between H-7 and H-3 as well as the chemical shift of H-6 at 7.04 ppm were consistent with  $\Delta^{2(6)}$  being the *E*-isomer. The stereochemistry of C-3 was determined as *R* based on the optical rotation  $[\alpha]^{25}_D$   $+116.0$  ( $c$  0.015,  $CHCl_3$ ) by comparison with related 4-hydroxybutanolides [31–33]. The NOESY correlation between H-3 and H-5 supported the 4*S* stereochemistry (Figure 3). TDDFT-ECD calculation was also sorted the (3*R*,4*S*) absolute configuration (Figure 4). Therefore, compound **6** (peltanolide F) was assigned as (2*E*,3*R*,4*S*)-3,4-dihydroxy-5-methyl-2-[(15*Z*)-15-icosenylidene]butanolide.

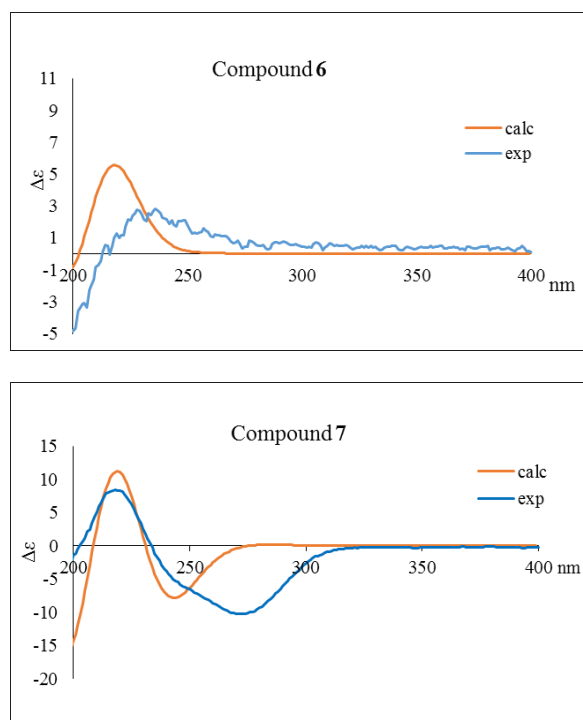


**Figure 4.** Experimental and calculated ECD spectra of compounds **6** and **7**.

Compound **7** has the molecular formula,  $C_{28}H_{50}O_4$ , based on the peak at  $m/z$  450.3702  $[M]^+$  in the HREIMS. All NMR data and EIMS fragment peaks (Figure 5) of **7** were identical to those of illigerone A [34]. However, the ECD spectrum of **7** exhibited a different Cotton effect from that of illigerone A, and TDDFT-ECD calculation was indicated the 3*R* absolute configuration (Figure 4). In addition, the experimental optical rotation,  $[\alpha]^{25}_D$   $-78.5$  ( $c$  0.03, acetonitrile), of **7** had a negative (levorotary) rather than positive (dextrorotary) value, as found with illigerone A [34]. We concluded that compound **7** (peltanolide G) is (3*R*,4*E*,20*Z*)-3-hydroxy-4-(2-methoxy-2-oxo)hexacos-4,20-dien-2-one, the enantiomer of illigerone A.

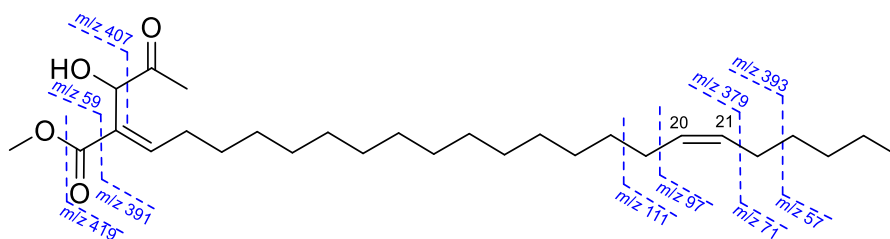


Figure 5. EIMS fragmentation of 7.

Compound **8** was obtained as a yellow solid, and its molecular formula was determined to be  $C_{27}H_{36}O_{13}$  on the HRFABMS ion at  $m/z$  591.2022  $[M + Na]^+$ . The  $^1H$  NMR data displayed five aromatic [ $\delta_H$  7.11 (1H, d,  $J = 8.2$  Hz), 6.92 (1H, d,  $J = 1.8$  Hz), 6.82 (1H, dd,  $J = 8.2, 1.8$  Hz), and 6.52 (2H, s, overlap)], two oxymethine [ $\delta_H$  4.63 (1H, d,  $J = 7.3$  Hz), 4.52 (1H, d,  $J = 8.2$  Hz)], four oxymethylene protons [ $\delta_H$  4.26 (1H, dd ( $J = 9.0, 4.6$  Hz), 3.92 (1H, m), 3.87 (1H, m), and 3.63 (1H, m)], three methoxy groups [ $\delta_H$  3.84 (6H, s), and 3.83 (3H, s)], and two methine protons [ $\delta_H$  2.53 (1H, m), 1.89 (1H, m)]. In addition, a glucopyranosyl anomeric proton was observed at  $\delta_H$  4.84 (1H, m). The  $^{13}C$  NMR spectrum showed 27 carbon signals, six from a glucose unit and three methoxy groups and the remaining 18 carbons from the lignan skeleton. The spectroscopic data of **8** resembled those of the known compound, (7*S*,8*R*,7'*S*,8'*S*)-4,9,7'-trihydroxy-3,3'-dimethoxy-7,9'-epoxylignan-4'-*O*- $\beta$ -*D*-glucopyranoside [35], except for the absence of the H-3 aromatic proton in the  $^1H$  NMR spectrum and the presence of an additional methoxy group in **8**. The HMBC (Figure 6) and NOESY (Figure 7) spectra agreed with this structure, and the observed ROESY correlations between H-7/H-9, H-8/H-7', and H-8'/H-9 (Figure 7) strongly suggested trans configurations of H-7/H-8 and H-8/H-8'. The CD spectrum of **8** showed positive Cotton effects at 237 nm and 274 nm (Figure 8), which were identical with those of the known compound [35]. Thus, the structure of **8** (peltaside A) was determined as (7*S*,8*R*,7'*S*,8'*S*)-4,9,7'-trihydroxy-3,5,3'-trimethoxy-7,9'-epoxylignan-4'-*O*- $\beta$ -*D*-glucopyranoside.

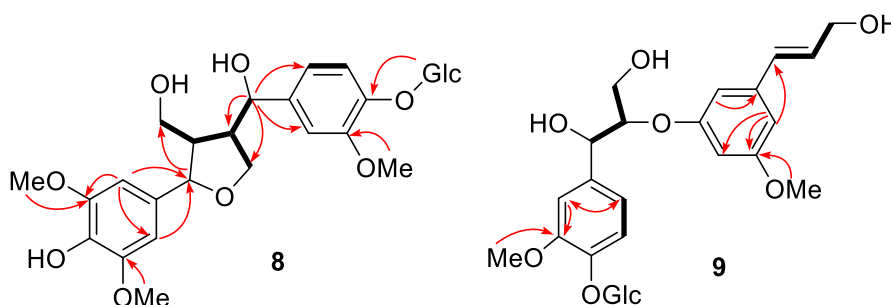


Figure 6. Selected HMBC correlations (arrows in red), COSY connectivities (bold lines) for **8** and **9**.

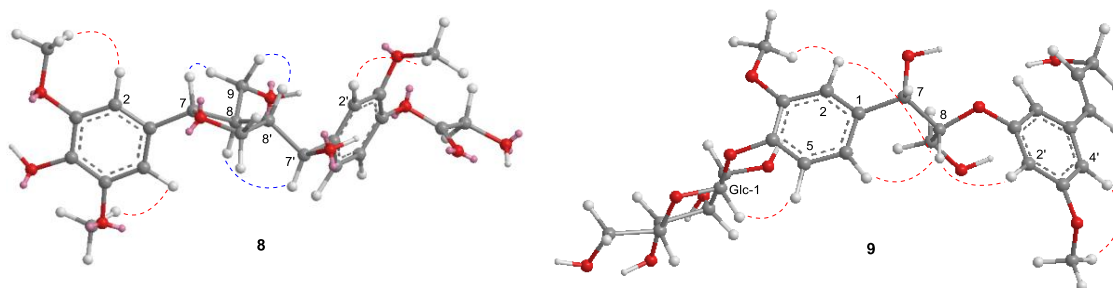
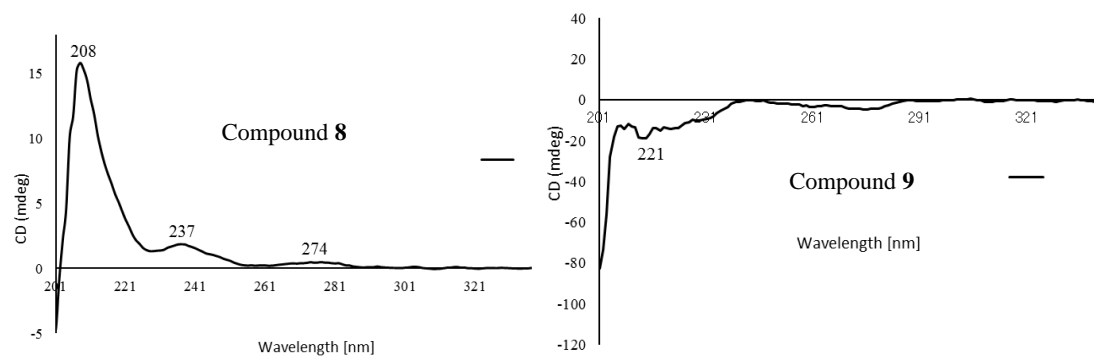


Figure 7. Key NOESY correlations (red lines) and Key ROESY correlations (blue lines) for **8** and **9**.



**Figure 8.** Experimental ECD spectra of compounds **8** and **9**.

Compound **9** was obtained as a yellow solid and its HRFABMS ( $m/z$  561.1958 [ $M + Na$ ] $^+$ ) indicated the molecular formula  $C_{26}H_{34}O_{12}$ . The  $^1H$  NMR spectrum of **9** displayed the signals for a trans-olefinic, two oxygenated methine, two oxygenated methylene, and six aromatic protons, as well as a  $\beta$ -glucose and two methoxy groups (Table 3). In addition, its  $^{13}C$ -NMR spectrum showed the signals for 26 carbons, including 12 aromatic, two methoxy, two olefinic, and six glucopyranosyl carbons (Table 3). The COSY, HMQC, HMBC, and NOESY spectra suggested that the glucopyranosyl moiety was attached to C-4 (Figures 5 and 6). The relative configuration between C-7 and C-8 was assigned as erythro based on the small coupling constant ( $J = 4.8$  Hz) in  $^1H$  NMR (Figure S57). The absolute configuration of **9**, which showed a negative Cotton effect at 221 nm in the CD spectrum (Figure 8), was determined to be 7*S*,8*R* via a comparison with that of reported analogues [36–38]. Hence, compound **9** (peltaside B) is (7*S*,8*R*,7'*E*)-7,9,9'-trihydroxy-3,5'-dimethoxy-8-3'-oxyneolign-7'-ene-4-*O*- $\beta$ -D-glucopyranoside.

**Table 3.**  $^1H$  and  $^{13}C$  NMR Spectroscopic Data of Compounds **8** and **9**.

Position	<b>8</b> (CD <sub>3</sub> OD)		<b>9</b> (CD <sub>3</sub> OD)	
	$\delta_C^a$	$\delta_H$ (J in Hz) <sup>b</sup>	$\delta_C^a$	$\delta_H$ (J in Hz) <sup>b</sup>
1	134.1		131.5	
2	104.6 <sup>c</sup>	6.52 s <sup>d</sup>	112.3	7.09 brs
3	149.3		147.4	
4	135.9		150.5	
5	149.3		120.6	7.06 d (8.2)
6	104.6 <sup>c</sup>	6.52 s <sup>d</sup>	121.1	6.96 dd (2.2, 8.2)
7	85.1	4.63 d (7.3)	74.9	4.85 overlap
8	53.7	1.89 m	85.9	4.36 m
9	62.3	3.87 m	62.2	3.82 m
		3.63 m		3.47 m
1'	139.5		137.8	
2'	112.2	6.92 d (1.8)	118.7 <sup>g</sup>	6.86 brs <sup>g</sup>
3'	150.7		149.2	
4'	147.5		118.7 <sup>g</sup>	6.86 brs <sup>g</sup>
5'	117.5	7.11 d (8.2)	151.2	
6'	120.9	6.82 dd (8.2, 1.8)	111.3	6.97 d (2.2)
7'	74.8	4.52 d (8.2)	132.9	6.52 d (15.4)
8'	50.7	2.53 m	111.3	6.27 dd (5.7, 15.4)
9'	76.2	4.26 dd (9.0, 4.6)	63.8	4.19 d (5.9)
		3.92 m		
3-OMe	56.9	3.84 s <sup>e</sup>	56.7	3.81 s
5-OMe	56.8	3.84 s <sup>e</sup>	56.5	3.79 s
3'-OMe	56.7	3.83 s		

Table 3. Cont.

Position	8 (CD <sub>3</sub> OD)		9 (CD <sub>3</sub> OD)	
	$\delta_C^a$	$\delta_H$ (J in Hz) <sup>b</sup>	$\delta_C^a$	$\delta_H$ (J in Hz) <sup>b</sup>
Glc-1	102.7	4.84 m	103.1	4.81 d (6.9)
Glc-2	74.9	3.4–3.8 m <sup>f</sup>	73.9	3.4–3.8 m <sup>h</sup>
Glc-3	78.2	3.4–3.8 m <sup>f</sup>	78.2	3.4–3.8 m <sup>h</sup>
Glc-4	71.4	3.4–3.8 m <sup>f</sup>	71.4	3.4–3.8 m <sup>h</sup>
Glc-5	77.9	3.4–3.8 m <sup>f</sup>	77.9	3.4–3.8 m <sup>h</sup>
Glc-6	62.5	3.4–3.8 m <sup>f</sup>	62.5	3.4–3.8 m <sup>h</sup>

<sup>a</sup> 100 Hz, <sup>b</sup> 400 Hz, <sup>c–h</sup> Overlapping signals.

## 2.2. Antiproliferative Activity of Isolated Compounds from *H. nymphaeifolia*

Compounds **1**, **2**, **8**, **10**, and **13–18** were evaluated for antiproliferative effects against five human tumor cell lines, A549 (lung carcinoma), MCF-7 (estrogen receptor-positive and HER2-negative breast cancer), MDA-MB-231 (triple negative breast cancer), KB (cervical cancer cell line HeLa derivative), and P-glycoprotein (P-gp)-overexpressing multidrug-resistant (MDR) KB subline, KB-VIN (Table 4). The remaining compounds were not tested due to insufficient quantities. Butanolide **10** slightly inhibited MCF-7 and KB-VIN tumor cell growth with an IC<sub>50</sub> value of 9  $\mu$ M. Both lignans **15** and **16** showed antiproliferative activity against chemosensitive A549 and MCF-7 tumor cell lines, while **16** was also active against MDA-MB-231. Interestingly, compounds **15** and **16** also displayed moderate activity against the MDR cell line (KB-VIN) with an IC<sub>50</sub> value of 5  $\mu$ M but were less active against its parent chemosensitive cell line (KB). Compounds **1**, **2**, **8**, **14** and **18** exhibited no activity against all tested cell lines. These results demonstrated that the CH<sub>3</sub>OH/CH<sub>2</sub>Cl<sub>2</sub> (1:1) extract of *H. nymphaeifolia* contained antiproliferative natural products, which showed broad spectrum against HTCLs including MDR cells and could also work synergistically against MDR cells.

Table 4. Antiproliferative Activity of the Isolated Compounds.

Compounds	Cell Lines <sup>a</sup> (IC <sub>50</sub> $\mu$ M) <sup>b</sup>				
	A549	MDA-MB-231	MCF-7	KB	KB-VIN
<b>1</b>	>40	22.5	>40	25.7	31.7
<b>2</b>	21.9	24.6	24.6	22.6	21.4
<b>8</b>	35.1	35.3	35.7	32.7	21.7
<b>10</b>	12.5	10.8	8.8	18.6	8.8
<b>13</b>	32.8	37.7	33.5	>40	8.7
<b>14</b>	23.2	32.9	32.8	23.2	19.9
<b>15</b>	8.1	20.8	6.8	20.3	5.4
<b>16</b>	5.7	8.2	8.1	12.6	5.3
<b>17</b>	37.8	>40	38.0	>40	8.2
<b>18</b>	>40	>40	>40	>40	>40
Paclitaxel (nM)	6.5	8.4	12.1	7.1	2213

<sup>a</sup> A549 (lung carcinoma), MDA-MB-231 (triple-negative breast cancer), MCF-7 (estrogen receptor-positive & HER2-negative breast cancer), KB (cervical cancer cell line HeLa derivative), KB-VIN (P-gp-overexpressing multidrug-resistant (MDR) subline of KB). <sup>b</sup> Antiproliferative activity expressed as IC<sub>50</sub> values for each cell line cultured with compound for 72 h, the concentration of compound that caused 50% reduction relative to untreated cells determined by the SRB assay. IC<sub>50</sub> of all compounds were calculated.

## 3. Materials and Methods

### 3.1. General Experimental Procedures

Infrared spectra (IR) were obtained with a Thermo Fisher Scientific (Waltham, MA, USA) NICOLET iS5 FT-TR spectrometer from samples in CHCl<sub>3</sub> and MeOH. NMR spectra were measured on JEOL

(Akishima, Tokyo, Japan) JNM-ECA600 and JNM-ECS400 spectrometers with tetramethylsilane as an internal standard, and chemical shifts are stated as  $\delta$  values. HRMS data were recorded on a JEOL JMS-700 Mstation (FAB or EI) mass spectrometer. Analytical and preparative TLC were carried out on precoated silica gel 60F254 and RP-18F254 plates (0.25 or 0.50 mm thickness; Merck, Darmstadt, Germany). MPLC was performed on a Combiflash  $R_f$  (Teledyne Isco, Lincoln, NE, USA) with silica gel and C18 cartridges (Biotage, Uppsala Sweden). Preparative HPLC was carried out with a GL Science (Shinjuku, Tokyo, Japan) recycling system (PU714 pump and UV702 UV-Vis detector) using an InertSustain C18 column (5  $\mu$ M, 20  $\times$  250 mm).

### 3.2. Plant Material

The crude  $\text{CH}_3\text{OH}/\text{CH}_2\text{Cl}_2$  (1:1) extract (#N053499) from fruit of *H. nymphaeifolia* (Presl) Kubitzki (originally identified as *H. peltata*), collected in Java (Indonesia) was provided by NCI/NIH. The plant was collected on May 25, 1992 in a sandy habitat in the Ujung Kulon Reserve by A. McDonald. A voucher specimen for the plant collection was deposited at the Smithsonian Institution (Washington, WA, USA) and voucher extracts were deposited at the NCI (Frederick, MD, USA) and Kanazawa University (Kanazawa, Ishikawa, Japan).

### 3.3. Extraction and Isolation

The crude extract N053499 (25.0 g) was dissolved in  $\text{CH}_3\text{OH}/\text{H}_2\text{O}$  (9:1) then partitioned with *n*-hexane, EtOAc, and *n*-BuOH, yielding *n*-hexane (17.4 g), EtOAc (3.94 g), *n*-BuOH (1.72 g), and  $\text{H}_2\text{O}$  (0.997 g) fractions. The EtOAc-soluble fraction was subjected to silica gel column chromatography (CC) with a gradient system [*n*-hexane/EtOAc 100:0 (500 mL)  $\rightarrow$  90:10 (500 mL)  $\rightarrow$  70:30 (1000 mL)  $\rightarrow$  50:50 (1000 mL)  $\rightarrow$  30:70 (1000 mL)  $\rightarrow$  10:90 (1000 mL)  $\rightarrow$  0:100 (500 mL)  $\rightarrow$  EtOAc/MeOH 50:50 (500 mL)  $\rightarrow$  MeOH (1000 mL)] to yield nine fractions, F1–F9. F3 (123 mg) was subjected to silica gel MPLC (RediSep Rf GOLD High Performance 4 g) eluted with *n*-hexane/EtOAc (9:1 to 0:1) to afford five subfractions 3a–e. Subfraction 3b (21.6 mg) was purified by repeated recycling reversed-phase preparative HPLC with  $\text{H}_2\text{O}/\text{MeOH}$  (1:19) to provide compounds **2** (2.2 mg), **3** (1.4 mg), and **10** (1.2 mg). F4 (77.9 mg) was subjected to silica gel CC eluted with  $\text{CH}_2\text{Cl}_2$  followed by MeOH to yield eight subfractions 4a–h. Subfraction 4d (1.0 mg) was further separated by preparative normal-phase TLC with  $\text{CH}_2\text{Cl}_2$  to afford compound **5** (0.4 mg). Subfraction 4f (4.6 mg) was purified by repeated recycling preparative HPLC with  $\text{H}_2\text{O}/\text{MeOH}$  (1:2) to afford compound **7** (0.6 mg). Subfraction 4h (54.0 mg) was purified by preparative normal-phase TLC with  $\text{CH}_2\text{Cl}_2/\text{EtOAc}$  (19:1) to afford compounds **13** (13.2 mg) and **15** (2.1 mg). F6 was subjected to silica gel CC eluted with  $\text{CH}_2\text{Cl}_2/\text{EtOAc}$  (19:1 to 0:1) followed by MeOH to obtain six subfractions, 6a–f. Subfraction 6b (37.5 mg) was purified by repeated recycling preparative HPLC with  $\text{H}_2\text{O}/\text{MeOH}$  (1:2) to afford compounds **12** (7.1 mg) and **16** (20.3 mg). Subfraction 6c (15.9 mg) was purified by repeated recycling preparative HPLC with  $\text{H}_2\text{O}/\text{MeOH}$  (1:2), to provide compound **17** (4.1 mg). The *n*-hexane fraction (12.0 g) was subjected to silica gel MPLC (RediSep Rf GOLD High Performance 120 g) with a gradient system [*n*-hexane/ $\text{CH}_2\text{Cl}_2$  1:1 (600 mL)  $\rightarrow$  2:3 (1400 mL)  $\rightarrow$  3:7 (1200 mL)  $\rightarrow$  4:1 (1400 mL)  $\rightarrow$   $\text{CH}_2\text{Cl}_2$  (1200 mL)  $\rightarrow$   $\text{CH}_2\text{Cl}_2/\text{EtOAc}$  1:1 (1000 mL)  $\rightarrow$  EtOAc (1000 mL)  $\rightarrow$  MeOH (1400 mL)] to yield 15 fractions, F1–F15. F6 (695 mg) was applied to silica gel MPLC (RediSep Rf GOLD High Performance 24 g) eluted with *n*-hexane/EtOAc (9:1 to 0:1) followed by MeOH to yield ten subfractions 6a–j. Subfraction 6e (197 mg) was subjected to silica gel CC eluted with *n*-hexane/EtOAc (2:3 to 0:1) followed by MeOH to yield 11 subfractions 6e1–11. Subfraction 6e5 (4.9 mg) was purified by preparative normal-phase TLC with *n*-hexane/ $\text{CH}_2\text{Cl}_2$  (3:1) to afford compound **6** (0.4 mg). F11 (1.12 g) was applied to silica gel MPLC (RediSep Rf GOLD High Performance 24 g) with *n*-hexane/EtOAc (9:1 to 0:1) followed by MeOH to yield seven subfractions 11a–g. Subfraction 11f (535 mg) was purified by MPLC on ODS-25 (YMC-DispoPack AT 12 g) with  $\text{H}_2\text{O}/\text{CH}_3\text{OH}$  (1:3), followed by recycling preparative HPLC with  $\text{H}_2\text{O}/\text{MeOH}$  (1:2) to afford compounds **13** (0.4 mg) and **14** (0.2 mg). F13 (1.35 g) was subjected to silica gel MPLC (RediSep Rf GOLD High Performance 24 g) with *n*-hexane/ $\text{CH}_2\text{Cl}_2/\text{EtOAc}$  (1:1:0 to 0:0:1) followed by MeOH to yield ten subfractions 13a–j.

Subfraction 13e (48.2 mg) was purified by ODS preparative TLC eluted three times using MeOH to afford compounds **1** (3.2 mg), **2** (1.1 mg), and **10** (1.0 mg). The *n*-BuOH-soluble fraction (1.72 g) was subjected to silica gel MPLC (RediSep R<sub>f</sub> GOLD High Performance 120 g) with a gradient system [CHCl<sub>3</sub>/MeOH 1:0 (1000 mL)→10:1 (1400 mL)→5:1 (1200 mL)→1:1 (1800 mL)→MeOH (1400 mL)] to yield nine fractions, F1–F9. F1 (147 mg) was subjected to silica gel CC eluted with CH<sub>2</sub>Cl<sub>2</sub>/EtOAc (1:0 to 0:1) followed by MeOH to obtain 14 subfractions, 1a–n. Compound **4** (0.3 mg) was obtained from subfraction 1e. Subfraction 1g (3.3 mg) was purified by preparative normal-phase TLC with CH<sub>2</sub>Cl<sub>2</sub>/EtOAc (95:5) to afford compound **10** (1.3 mg). Subfraction 1k was purified by recycling preparative HPLC with H<sub>2</sub>O/MeOH (1:3) to afford compounds **11** (1.8 mg), **14** (0.3 mg), and **17** (0.4 mg). F2 (44.3 mg) was subjected to silica gel CC eluted with CH<sub>2</sub>Cl<sub>2</sub>/EtOAc (9:0 to 0:1) followed by MeOH to obtain nine subfractions, 2a–i. Subfraction 2b (1.1 mg) was purified by ODS preparative TLC eluted three times using H<sub>2</sub>O/MeOH (1:8) to yield compound **13** (0.6 mg). F3 (33.8 mg) was purified by preparative normal-phase TLC with CHCl<sub>3</sub>/MeOH (9:1) to afford compound **8** (1.0 mg). F5 (149 mg) was subjected to silica gel CC eluted with CH<sub>2</sub>Cl<sub>2</sub>/MeOH (10:1 to 1:1) followed by MeOH to obtain seven subfractions, 5a–g. Subfraction 5d (75.6 mg) was purified by MPLC on ODS-25 (YMC-DispoPack AT 12 g) with H<sub>2</sub>O/MeOH (1:3), followed by recycling preparative HPLC with H<sub>2</sub>O/MeOH (2:3) to afford compounds **9** (1.3 mg), **18** (2.3 mg), **19** (1.0 mg), and **20** (1.2 mg).

### 3.3.1. Peltanolide A (**1**)

Yellow amorphous solid;  $[\alpha]_D^{25} +27.3$  (*c* 0.075, CHCl<sub>3</sub>); IR  $\nu_{\max}$  (CHCl<sub>3</sub>) cm<sup>-1</sup> 2923, 2853, 2017, 1733, 1457, 1278, 1219; <sup>1</sup>H and <sup>13</sup>C NMR, Tables 1 and 2; HREIMS *m/z* 390.3137 [M]<sup>+</sup> (calcd for C<sub>25</sub>H<sub>42</sub>O<sub>3</sub>, 390.3134).

### 3.3.2. Peltanolide B (**2**)

Yellow amorphous solid;  $[\alpha]_D^{25} +26.1$  (*c* 0.12, CHCl<sub>3</sub>); IR  $\nu_{\max}$  (CHCl<sub>3</sub>) cm<sup>-1</sup> 2923, 2852, 1731, 1464, 1265, 1074; <sup>1</sup>H and <sup>13</sup>C NMR, Tables 1 and 2; HREIMS *m/z* 446.3743 [M]<sup>+</sup> (calcd for C<sub>29</sub>H<sub>51</sub>O<sub>3</sub>, 446.3760).

### 3.3.3. Peltanolide C (**3**)

Colorless oil;  $[\alpha]_D^{25} +26.0$  (*c* 0.07, CHCl<sub>3</sub>); IR  $\nu_{\max}$  (CHCl<sub>3</sub>) cm<sup>-1</sup> 2916, 2849, 2016, 1750, 1678, 1470, 1278, 1184; <sup>1</sup>H and <sup>13</sup>C NMR, Tables 1 and 2; HREIMS *m/z* 392.3302 [M]<sup>+</sup> (calcd for C<sub>25</sub>H<sub>44</sub>O<sub>3</sub>, 392.3290).

### 3.3.4. Peltanolide D (**4**)

Yellow amorphous solid;  $[\alpha]_D^{25} -29.7$  (*c* 0.02, CHCl<sub>3</sub>); IR  $\nu_{\max}$  (CHCl<sub>3</sub>) cm<sup>-1</sup> 2923, 2852, 1783, 1733, 1465, 1373, 1287; <sup>1</sup>H and <sup>13</sup>C NMR, Tables 1 and 2; HRFABMS *m/z* 441.3357 [M + Na]<sup>+</sup> (calcd for C<sub>27</sub>H<sub>46</sub>O<sub>3</sub>Na, 441.3345).

### 3.3.5. Peltanolide E (**5**)

Yellow amorphous solid;  $[\alpha]_D^{25} -21.1$  (*c* 0.015, CHCl<sub>3</sub>); IR  $\nu_{\max}$  (CHCl<sub>3</sub>) cm<sup>-1</sup> 2922, 2852, 2017, 1770, 1731, 1557, 1458, 1375, 1287; <sup>1</sup>H and <sup>13</sup>C NMR, Tables 1 and 2; HREIMS *m/z* 446.3749 [M]<sup>+</sup> (calcd for C<sub>29</sub>H<sub>50</sub>O<sub>3</sub>, 446.3760).

### 3.3.6. Peltanolide F (**6**)

Colorless oil;  $[\alpha]_D^{25} +116.0$  (*c* 0.015, CHCl<sub>3</sub>); IR  $\nu_{\max}$  (CHCl<sub>3</sub>) cm<sup>-1</sup> 2923, 2852, 1733, 1558, 1540, 1456, 1287; <sup>1</sup>H and <sup>13</sup>C NMR, Tables 1 and 2; HREIMS *m/z* 408.3230 [M]<sup>+</sup> (calcd for C<sub>25</sub>H<sub>44</sub>O<sub>4</sub>, 408.3240).

### 3.3.7. Peltanolide G (7)

Colorless oil;  $[\alpha]_D^{25}$   $-78.5$  ( $c$  0.03, acetonitrile); IR  $\nu_{\max}$  ( $\text{CHCl}_3$ )  $\text{cm}^{-1}$  2922, 2852, 2016, 1717, 1669, 1558, 1456, 1436;  $^1\text{H}$  and  $^{13}\text{C}$  NMR, Tables 1 and 2; HREIMS  $m/z$  450.3702  $[\text{M}]^+$  (calcd for  $\text{C}_{28}\text{H}_{50}\text{O}_4$ , 450.3709).

### 3.3.8. Peltaside A (8)

Yellow solid;  $[\alpha]_D^{25}$   $+5.6$  ( $c$  0.055, MeOH); IR  $\nu_{\max}$  ( $\text{CHCl}_3$ )  $\text{cm}^{-1}$  3330, 2945, 2833, 1645, 1514, 1450, 1112;  $^1\text{H}$  and  $^{13}\text{C}$  NMR, Table 3; HRFABMS  $m/z$  591.2022  $[\text{M} + \text{Na}]^+$  (calcd for  $\text{C}_{27}\text{H}_{36}\text{O}_{13}\text{Na}$ , 591.2054).

### 3.3.9. Peltaside B (9)

Yellow solid;  $[\alpha]_D^{25}$   $-71.8$  ( $c$  0.065, MeOH); IR  $\nu_{\max}$  ( $\text{CHCl}_3$ )  $\text{cm}^{-1}$  3386, 3293, 1657, 1511, 1265;  $^1\text{H}$  and  $^{13}\text{C}$  NMR, Table 3; HRFABMS  $m/z$  561.1958  $[\text{M} + \text{Na}]^+$  (calcd for  $\text{C}_{26}\text{H}_{34}\text{O}_{12}\text{Na}$ , 561.1948).

## 3.4. Calculation of ECD Spectra

Preliminary conformational analysis for each compound was carried out by using CONFLEX8 with the MMFF94 force field. The conformers were further optimized in MeCN by density functional theory (DFT) method with the B3LYP functional and 6–31(d) basis set. The ECD spectrum was calculated by the time-dependent DFT (TDDFT) method with the CAM-B3LYP functional and TZVP basis set. The calculation was completed by the use of conformers within 2 kcal/mol predicted in MeCN. The solvent effect was introduced by the conductor-like polarizable continuum model (CPCM). The DFT optimization and TDDFT-ECD calculation were performed using Gaussian09 (Gaussian, Inc., Wallingford, CT, USA). The calculated spectrum was displayed by GaussView 5.0.920 with the peak half-width at half height being 0.333 eV. The Boltzmann-averaged spectrum at 298.15K was calculated using Excel 2016 (Microsoft Co., Redmond, WA, USA). The calculations were re-optimized according to the literature [39].

## 3.5. Assay for Antiproliferative Activity

Antiproliferative activity of the compounds was determined by the sulforhodamine B (SRB) assay as described previously [40]. Briefly, cell suspensions were seeded on 96-well microtiter plates at a density of 4000–12,000 cells per well and cultured for 72 h with test compound. The cells were fixed in 10% trichloroacetic acid and then stained with 0.04% SRB. The absorbance at 515 nm of 10 mM Tris base-solubilized protein-bound dye was measured using a microplate reader (ELx800, BioTek, Winooski, VT, U.S) operated by Gen5 software (BioTek).  $\text{IC}_{50}$  data were calculated statistically (MS Excel) from at least three independent experiments performed with duplication ( $n = 6$ ). All human tumor cell lines, except KB-VIN, were obtained from the Lineberger Comprehensive Cancer Center (UNC-CH, Chapel Hill, NC, USA) or from ATCC (Manassas, VA, USA). KB-VIN was a generous gift from Professor Y.-C. Cheng of Yale University (New Haven, CT, USA).

## 4. Conclusions

As part of our continuing investigation of rainforest plants, we conducted a thorough study to identify new chemical compounds to supplement the reported phytochemical research on *H. nymphaeifolia*. Consequently, a  $\text{CH}_3\text{OH}/\text{CH}_2\text{Cl}_2$  (1:1) extract of *H. nymphaeifolia* (N053499) provided by NCI yielded seven new butanolides, peltanolides A–G (1–7), and two new lignan glycosides, peltasides A (8) and B (9), as well as eleven known compounds 10–20. This is the first report to identify butanolides and lignan glucosides from this genus. The evaluation of antiproliferative activity against human tumor cell lines revealed that lignans 15 and 16 were slightly active against chemosensitive tumor cell lines A549 and MCF-7, respectively. Interestingly, both compounds displayed significant activity with  $\text{IC}_{50}$  valued of 5  $\mu\text{M}$  against a P-glycoprotein overexpressing MDR tumor cell line (KB-VIN) although they were less active against its parent chemosensitive cell line (KB).

**Supplementary Materials:** NMR spectra and HRMS of new compounds are available online at <http://www.mdpi.com/1420-3049/24/21/4005/s1>.

**Author Contributions:** S.A., Y.S.; investigation, performed the chemical experiments and data collection, S.F.; ECD calculation and analysis, M.G.; investigation, performed cytotoxic experiments using SRB assay, M.G., K.M., D.J.N, B.R.O. K.-H.L.; editing and guidance, K.N.-G; writing, conceptualization, and supervision.

**Funding:** This study was supported by JSPS KAKENHI Grant Number JP25293024, awarded to K.N.G. This work was also supported partially by NIH grant CA177584 from the National Cancer Institute, awarded to K.H.L., as well as the Eshelman Institute for Innovation, Chapel Hill, North Carolina, awarded to M.G. The content of this publication does not necessarily reflect the views or policies of the Department of Health and Human Services, nor does mention of trade names, commercial products, or organizations imply endorsement by the U.S. Government.

**Acknowledgments:** We appreciate critical comments, suggestions, and editing on the manuscript by Susan L. Morris-Natschke (UNC-CH).

**Conflicts of Interest:** The authors declare no conflict of interest.

## References

1. Lakshmi, V.; Pandey, K.; Mishra, S.K.; Srivastava, S.; Mishra, M.; Agarwa, S.K. An overview of family *Hernandiaceae*. *Rec. Nat. Prod.* **2009**, *3*, 1–22.
2. Pettit, G.R.; Meng, Y.H.; Gearing, R.P.; Herald, D.L.; Pettit, R.K.; Doubek, D.L.; Chapuis, J.C.; Tackett, L.P. Antineoplastic Agents. 522. *Hernandia peltata* (Malaysia) and *Hernandia nymphaeifolia* (Republic of Maldives). *J. Nat. Prod.* **2004**, *67*, 214–220. [[CrossRef](#)] [[PubMed](#)]
3. Udino, L.; Abaul, J.; Bourgeois, P.; Corrichon, L.; Duran, H.; Zedde, C. Lignans from the seeds of *Hernandia sonora*. *Planta Med.* **1999**, *65*, 279–281. [[CrossRef](#)] [[PubMed](#)]
4. Chalandre, M.C.; Bruneton, J.; Cabalion, P.; Guinaudeau, H. Hernandiaceae. XII. Aporphine-benzylisoquinoline dimers isolated from *Hernandia peltata*. *Can. J. Chem.* **1986**, *64*, 123–126. [[CrossRef](#)]
5. Wei, C.Y.; Wang, S.W.; Ye, J.W.; Hwang, T.L.; Cheng, M.J.; Sung, P.J.; Chang, T.H.; Chen, J.J. New anti-inflammatory aporphine and lignan derivatives from the root wood of *Hernandia nymphaeifolia*. *Molecules* **2018**, *23*, 2286. [[CrossRef](#)]
6. Lavault, M.; Cabalion, P.; Bruneton, J. Study on Hernandiaceae. IV. Alkaloids of *Hernandia peltata*. *Planta Med.* **1982**, *46*, 119–121. [[CrossRef](#)]
7. Chen, J.J.; Tsai, I.L.; Chen, I.S. New Oxoaporphine Alkaloids from *Hernandia nymphaeifolia*. *J. Nat. Prod.* **1996**, *59*, 156–158. [[CrossRef](#)]
8. Chen, J.J.; Ishikawa, T.; Duh, C.Y.; Tsai, I.L.; Chen, I.S. New dimeric aporphine alkaloids and cytotoxic constituents of *Hernandia nymphaeifolia*. *Planta Med.* **1996**, *62*, 528–533. [[CrossRef](#)]
9. Angerhofer, C.K.; Guinaudeau, H.; Wongpanich, V.; Pezzuto, J.M.; Cordell, G.A. Antiplasmodial and cytotoxic activity of natural bisbenzylisoquinoline alkaloids. *J. Nat. Prod.* **1999**, *62*, 59–66. [[CrossRef](#)]
10. Rasoanaivo, R.; Urverg, R.; Rafatro, H.; Ramanitrahasimbola, D.; Palazzino, G.; Galeffi, C.; Nicoletti, M. Alkaloids of *Hernandia voyronii*. Chloroquine-potentiating activity and structure elucidation of herveline D. *Planta Med.* **1998**, *64*, 58–62. [[CrossRef](#)]
11. Dittmar, A. The effectiveness of *Hernandia* spp. (Hernandiaceae) in traditional Samoan medicine and according to scientific analyses. *J. Ethnopharmacol.* **1991**, *33*, 243–251. [[CrossRef](#)]
12. Bruneton, J.; Shamma, M.; Minard, R.D.; Freyer, A.J.; Guinaudeau, H. Novel biogenetic pathways from (+)-reticuline. Three dimeric alkaloids: (+)-vanuatine, (+)-vateamine, and (+)-malekulatine. *J. Org. Chem.* **1983**, *48*, 3957–3960. [[CrossRef](#)]
13. Chen, I.S.; Chen, J.J.; Duh, C.Y.; Tsai, I.L. Cytotoxic lignans from Formosan *Hernandia nymphaeifolia*. *Phytochemistry* **1997**, *45*, 991–996. [[CrossRef](#)]
14. Chen, I.J.; Chang, Y.L.; Teng, C.M.; Chen, I.S. Anti-platelet aggregation alkaloids and lignans from *Hernandia nymphaeifolia*. *Planta Med.* **2000**, *66*, 251–256. [[CrossRef](#)] [[PubMed](#)]
15. Yoder, B.J.; Cao, S.; Norris, A.; Miller, J.S.; Ratovoson, F.; Andriantsiferana, R.; Rasamison, V.E.; Kingston, D.G.I. Tambouranolide, a new cytotoxic hydroxybutanolide from a *Tambourissa* sp. (Monimiaceae). *Nat. Prod. Res.* **2007**, *21*, 37–41. [[CrossRef](#)] [[PubMed](#)]

16. Muto, N.; Tomokuni, T.; Haramoto, M.; Tatemoto, H.; Nakanishi, T.; Inatomi, Y.; Murata, H.; Inada, A. Isolation of apoptosis- and differentiation-inducing substances toward human promyelocytic leukemia HL-60 cells from leaves of *Juniperus taxifolia*. *Biosci. Biotechnol. Biochem.* **2008**, *72*, 477–484. [[CrossRef](#)] [[PubMed](#)]
17. Trazzi, G.; André, M.F.; Coelho, F.J. Diastereoselective synthesis of  $\beta$ -piperonyl- $\gamma$ -butyrolactones from Morita-Baylis-Hillman adducts. Highly efficient synthesis of ( $\pm$ )-yatein, ( $\pm$ )-podorhizol and ( $\pm$ )-*epi*-podorhizol. *Braz. Chem. Soc.* **2010**, *21*, 2327–2339. [[CrossRef](#)]
18. Okunishi, T.; Umezawa, T.; Shimada, M. Enantiomeric compositions and biosynthesis of *Wikstroemia sikokiana* lignans. *J. Wood Sci.* **2000**, *46*, 234–242. [[CrossRef](#)]
19. Li, N.; Wu, J.L.; Sakai, J.I.; Ando, M. Dibenzylbutyrolactone and Dibenzylbutanediol Lignans from *Peperomia duclouxii*. *J. Nat. Prod.* **2003**, *66*, 1421–1426. [[CrossRef](#)]
20. Ahmed, A.A.; Mahmoud, A.A.; Ali, E.T.; Tzakou, O.; Couladis, M.; Mabry, T.J.; Gáti, T.; Tóth, G. Two highly oxygenated eudesmanes and ten lignans from *Achillea holosericea*. *Phytochemistry* **2002**, *59*, 851–856. [[CrossRef](#)]
21. Iida, T.; Nakano, M.; Ito, K. Hydroperoxysequiterpene and lignan constituents of *Magnolia kobus*. *Phytochemistry* **1982**, *21*, 673–675. [[CrossRef](#)]
22. Asikin, Y.; Takahashi, M.; Mizu, M.; Takara, K.; Okua, H.; Wada, K. DNA damage protection against free radicals of two antioxidant neolignan glucosides from sugarcane molasses. *J. Sci. Food Agric.* **2016**, *96*, 1209–1215. [[CrossRef](#)] [[PubMed](#)]
23. Calis, I.; Kirmizibekmez, H.; Beutler, J.A.; Donmez, A.A.; Yalc, F.N.; Kilic, I.E.; Ozlap, M.; Ruedi, P.; Tasdemir, D. Secondary metabolites of *Phlomis viscosa* and their biological activities. *Turk. J. Chem.* **2005**, *29*, 71–81.
24. Sugiyama, M.; Kikuchi, M. Phenylethanoid glycosides from *Osmanthus asiaticus*. *Phytochemistry* **1993**, *32*, 1553–1555. [[CrossRef](#)]
25. Seki, K.; Sasaki, T.; Wano, S.; Haga, K.; Kaneko, R. Linderanolides and isolinderanolides, ten butanolides from *Lindera glauca*. *Phytochemistry* **1995**, *40*, 1175–1181. [[CrossRef](#)]
26. Anderson, J.E.; Ma, W.; Smith, D.L.; Chang, C.J.; Mclaughlin, J.L. Biologically active  $\gamma$ -lactones and methylketoalkenes from *Lindera benzoin*. *J. Nat. Prod.* **1992**, *55*, 71–83. [[CrossRef](#)]
27. Tamura, S.; Doke, S.; Murakami, N. Total synthesis of peumusolide A, NES non-antagonistic inhibitor for nuclear export of MEK. *Tetrahedron* **2010**, *66*, 8476–8480. [[CrossRef](#)]
28. Tamura, S.; Tonokawa, M.; Murakami, N. Stereo-controlled synthesis of analogs of peumusolide A, NES non-antagonistic inhibitor for nuclear export of MEK. *Tetrahedron Lett.* **2010**, *51*, 3134–3137. [[CrossRef](#)]
29. Tsenga, M.; Su, Y.S.; Cheng, M.J.; Liu, T.W.; Chen, I.S.; Wu, M.D.; Chang, H.S.; Yuan, G.F. Chemical constituents from a soil-derived actinomycete, *Actinomadura miaoliensis* BCRC 16873, and their inhibitory activities on lipopolysaccharide-induced tumor necrosis factor production. *Chem. Biodivers.* **2013**, *10*, 303–312. [[CrossRef](#)]
30. Tanaka, H.; Takaya, Y.; Toyoda, J.; Yasuda, T.; Sato, M.; Murata, J.; Murata, H.; Kaburagi, K.; Iida, O.; Sugiyama, K.; et al. Two new butanolides from the roots of *Litsea acuminata*. *Phytochemistry Lett.* **2015**, *11*, 32–36. [[CrossRef](#)]
31. Cheng, H.I.; Lin, W.Y.; Duh, C.Y.; Lee, K.H.; Tsai, I.L.; Chen, I.S. New cytotoxic butanolides from *Litsea acutivena*. *J. Nat. Prod.* **2001**, *64*, 1502–1505. [[CrossRef](#)] [[PubMed](#)]
32. Juan, C.; Martinez, V.; Yoshida, M.; Gottlieb, O.R. The chemistry of Brazilian Lauraceae. Part LXI.  $\omega$ -Ethyl,  $\omega$ -ethenyl and  $\omega$ -ethynyl- $\alpha$ -alkylidene- $\gamma$ -lactones from *Clinostemon mahuba*. *Phytochemistry* **1981**, *20*, 459–464. [[CrossRef](#)]
33. Takeda, K.I.; Sakurawi, K.; Ishi, H. Components of the Lauraceae family. I. New lactonic compounds from *Litsea japonica*. *Tetrahedron* **1972**, *28*, 3757–3766. [[CrossRef](#)]
34. Li, X.J.; Dong, J.W.; Cai, L.; Wang, J.P.; Yu, N.X.; Ding, Z.T. Illigerones A and B, two new long-chain secobutanolides from *Illigera henryi* W. W. Sm. *Phytochem. Lett.* **2017**, *19*, 181–186. [[CrossRef](#)]
35. Yang, Y.N.; Huang, X.Y.; Feng, Z.M.; Jiang, J.S.; Zhang, P.C. Hepatoprotective Activity of Twelve Novel 7'-Hydroxy Lignan Glucosides from *Arctii Fructus*. *J. Agric. Food Chem.* **2014**, *62*, 9095–9102. [[CrossRef](#)] [[PubMed](#)]
36. Greca, M.D.; Molinaro, A.; Monaco, P.; Previtera, L. Neolignans from *Arum italicum*. *Phytochemistry* **1994**, *35*, 777–779. [[CrossRef](#)]

37. Arnoldi, A.; Merlini, L. Asymmetric synthesis of 3-methyl-2-phenyl-1,4-benzodioxanes. Absolute configuration of the neolignans eusiderin and eusiderin C and D. *J. Chem. Soc. Perkin Trans. I* **1985**, 2555–2557. [[CrossRef](#)]
38. Gan, M.; Zhang, Y.L.; Lin, S.; Liu, M.T.; Song, W.X.; Zi, J.C.; Yang, Y.C.; Fan, X.N.; Shi, J.G.; Hu, J.F.; et al. Glycosides from the root of *Iodes cirrhosa*. *J. Nat. Prod.* **2008**, *71*, 647–654. [[CrossRef](#)]
39. Pascitelli, G.; Bruhn, T. Good Computational Practice in the Assignment of Absolute Configurations by TDDFT Calculations of ECD Spectra. *Chirality* **2016**, *28*, 466–474. [[CrossRef](#)]
40. Nakagawa-Goto, K.; Oda, A.; Hamel, E.; Ohkoshi, E.; Lee, K.H.; Goto, M. Development of a novel class of tubulin inhibitors from desmosdumotin B with a hydroxylated bicyclic B-ring. *J. Med. Chem.* **2015**, *58*, 2378–2389. [[CrossRef](#)]

**Sample Availability:** Not available.



© 2019 by the authors. Licensee MDPI, Basel, Switzerland. This article is an open access article distributed under the terms and conditions of the Creative Commons Attribution (CC BY) license (<http://creativecommons.org/licenses/by/4.0/>).